

Response letter

Dear Editor:

Firstly, we are very sincerely sorry to have uploaded the wrong version in the previous submission. We have now uploaded the newly manuscript and response letter. On behalf of my co-authors, we thank you very much for giving us an opportunity to revise our manuscript, we appreciate editor and reviewers very much for their positive and constructive comments and suggestions on our manuscript entitled “A fast approximation for 1D Inversion of Transient Electromagnetic Data by BP Neural Network and improved Particle Swarm Optimization”. (MS No: npg-2019-36).

We have studied reviewer’s comments carefully and have made revision which marked in red in the paper. We have tried our best to revise our manuscript according to the comments. Attached please find the revised version, which we would like to submit for your kind consideration.

We would like to express our great appreciation to you and reviewers for comments on our paper. Looking forward to hearing from you.

Thank you and best regards.

Yours sincerely,

Huaiqing Zhang

The State Key Laboratory of Transmission Equipment and System Safety and Electrical New Technology, Chongqing University, Chongqing, China

Tel: + 86 13752954568

E_mail: zhanghuaiqing@cqu.edu.cn

Dear Editors and Reviewers:

Thank you for your letter and for the reviewers' comments concerning our manuscript entitled "A fast approximation for 1D Inversion of Transient Electromagnetic Data by BP Neural Network and improved Particle Swarm Optimization". (MS No: npg-2019-36). Those comments are all valuable and very helpful for revising and improving our paper, as well as the important guiding significance to our researches. We have studied comments carefully and have made correction which we hope meet with approval. Revised portion are marked in red in the paper. The main corrections in the paper and the responds to the reviewer's comments are as flowing:

For your guidance, itemized response to each review's comments is appended below.

Dear Norbert Marwan:

Comments:

1) The newly uploaded manuscript and response letter is the same as for the previous version. Perhaps the authors have uploaded the wrong version?

(1) We are very sincerely sorry to have uploaded the wrong version in the previous submission. We have now uploaded the newly manuscript and response letter, and apologize for any inconvenience again.

Reviewer #1:

Dear reviewers:

Comments:

1) In some sentences, the use of geoelectrical parameters instead of geoelectric parameters can be more suitable. Please also depict in the introduction of the paper what are these parameters. For instance, ...geoelectrical parameters consisting of the resistivities and thicknesses of the layers...

2) Based on equation 14 in the text, Ts and Os are unitless.

3) Considering the y-label of Fig. 4, I can not see any explanations related to the Rastrigin benchmark function used in your theoretical case. It would be nice if you also provided a clear version of the manuscript.

4) You declare that Fig. 3 shows one of the evolutionary training error curves. Considering the sentence given below, you should clearly verify whether this finding is also valid for each independent run of the algorithms.

"However, the COPSO-BP has better convergence rate and optimization efficiency in the early stage in Fig.3."

5) Please update Fig. 12 by adding the noise content to the theoretical curve.

6) How did you obtain error values less than the noise content added to the theoretical data?

7) Considering Fig. 14 that present the results of two approaches, the same resistivity range and contour interval must be used.

8) You should also mention in the paper which model parameters did you obtain through the PSO part of the algorithm at the end of 30 iterations. What are their error values as initial estimates requiring by the BP approach?

9) The title of the paper should be reconsidered by the authors. What does it mean "Transient Electromagnetic Inversion". Think about "A fast approximation for 1D Inversion of Transient

Electromagnetic Data by ..” or etc.

1- Reply:

1-In some sentences, the use of geoelectrical parameters instead of geoelectric parameters can be more suitable. Please also depict in the introduction of the paper what are these parameters. For instance, ...geoelectrical parameters consisting of the resistivities and thicknesses of the layers...

(1) Special thanks to your great comments on this manuscript. As you can see, some of the terminology as 'geoelectric parameters' that used in the paper is not very suitable. We have already made changes in the manuscript, some of which are modified as follows:

All the **geoelectrical parameters** and the forward model relations are implied in the weight and threshold parameters of ANN.

For BP structure, the output nodes are determined by the number of inversion **geoelectrical parameters**,.....

The BP training samples which is a series of $H_z(t)$ for different **geoelectrical parameters** were generated by TEM forward model.

In addition, in order to facilitate the reader's understanding, the geoelectric parameters involved in the introduction of the paper have been elaborated accordingly, as follows:

Transient electromagnetic (TEM) method applies the secondary receiving voltage induced by the rapid switching off pulse current, and then deduces **the geoelectrical parameters consisting of the resistivities and thicknesses of the layers**.

2-Based on equation 14 in the text, Ts and Os are unitless.

(2) As you can see, the Ts and Os in equation 14 are unitless. In the paper, in order to evaluate the effect of model training, the training error expression in equation 14 is used: $E = \frac{1}{S} \sum_s (T_s - O_s)^2$, where

S is the number of training samples, and Ts and Os are the expected output value and predicted output value of training sample S, respectively, which as the theoretical value $f(x)$ and the predicted value $f(x)$ of the *Rosenbrock and Bohachevsky* testing functions in the Testing Algorithm part, therefore Ts and Os only represent values without units.

(1) *Rosenbrock* function:

$$f_1(x) = 100 \times (x_1^2 - x_2)^2 + (1 - x_1)^2, x_i \in [-10, 10], i = 1, 2 \quad (1)$$

(2) *Bohachevsky* function:

$$f_2(x) = x_1^2 + x_2^3 - x_1 x_2 x_3 + x_3 - \sin(x_2^2) - \cos(x_1 x_3^2), x_i \in [-2\pi, 2\pi], i = 1, 2, 3 \quad (2)$$

3- Considering the y-label of Fig. 4, I can not see any explanations related to the Rastrigin benchmark function used in your theoretical case. It would be nice if you also provided a clear version of the manuscript.

(3) We are very sincerely sorry that the Rosenbrock and Bohachevsky testing functions have not been explained in detail in the theoretical case. In order to facilitate the reader's understanding of the article, we have made corresponding modifications in the Algorithm Testing section as follows:

In order to investigate the COPSO-BP performance and reliability, Rosenbrock and Bohachevsky testing functions were adopted, which are typical non-convex functions and mainly to evaluate the performance of unconstrained algorithms. However, due to the random nature of the function, it is not easy to solve and has a global minimum function value $f(x) = 0$.

Moreover, the Rosenbrock function is described in more detail: Rosenbrock function is a very classic function test problem in unconstrained optimization theory and method, it is an important tool to measure the advantages and disadvantages of unconstrained algorithms. In the field of numerical optimization, the function was proposed by Howard.H. Rosenbrock in 1960. In addition, it is a typical non-convex function that mainly used to optimize the performance test of the algorithm, but it is not easy to solve. And the fitness of the function is very simple in the terrain away from the most advantageous area, but the area near the most advantageous is banana-shaped. There is a strong correlation between variables, and gradient information often misleads the search direction of the algorithm. Each contour of the Rosenbrock function is roughly parabolic, and its global minimum is also in a parabolic valley (banana-type valley). It is easy to find this valley, but which is quite difficult to find the minimum of the whole domain that since the value in the valley does not change much. Among them, the Rosenbrock function could find the global minimum value of 0 at $(x_1, x_2, \dots, x_n) = (1, 1, \dots, 1)$, but due to its random nature, any optimization algorithm based on the falling gradient fails to find the global minimum value. A three-dimensional map of the Rosenbrock function of two of these variables is shown in Figure 1.

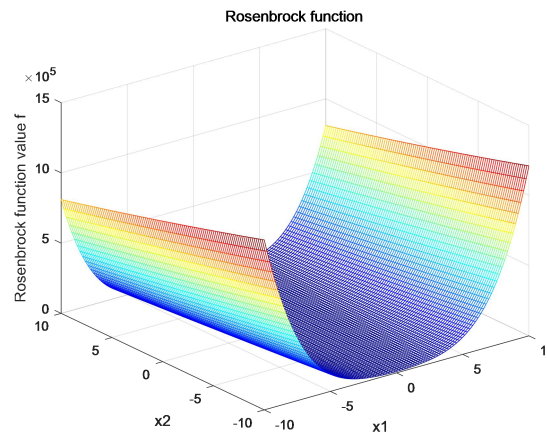


Fig.1 3D diagram of the Rosenbrock function

4- You declare that Fig. 3 shows one of the evolutionary training error curves. Considering the sentence given below, you should clearly verify whether this finding is also valid for each independent run of the algorithms.

“However, the COPSO-BP has better convergence rate and optimization efficiency in the early stage in Fig.3.”

(4) In the Algorithm testing part of the paper, in order to verify the accuracy and stability of the algorithm, 20 independent experiments were carried out. The experiments show that the results predicted by the COPSO-BP algorithm are better than those of SPSO-BP in almost all experiments. Figure 2 below shows the results of the three runs of the Rosenbrock function by the SPSO-BP and the COPSO-BP. And from Figure 2 and Table 1, it can be seen that after 20 independent experiments, whether it is the Rosenbrock test function or the Bohachevsky test function, the optimal value and average value predicted by the COPSO-BP algorithm are better than SPSO-BP results, so that COPSO-BP has better convergence rate and optimization efficiency. However, the length of the article is limited, and it is not listed one by one. The corresponding supplements in the manuscript are as follows:

One of the evolutionary training error curves (select one in 20 times randomly) were shown in Fig.3,

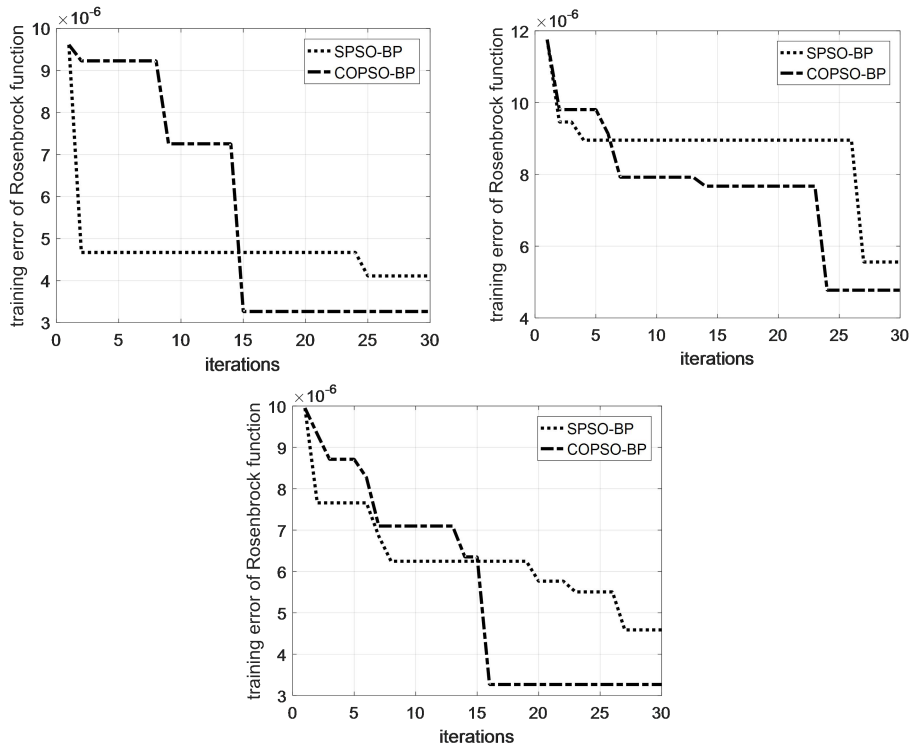


Fig. 2 Training error curves of SPSO-BP and COPSO-BP algorithms

Table.1 Comparison of SPSO-BP and COPSO-BP algorithm for testing functions

Testing functions	SPSO-BP		COPSO-BP	
	Average value	Optimal value	Average value	Optimal value
<i>Rosenbrock</i>	2.375e-3	2.300e-5	1.201e-3	2.410e-06
<i>Bohachevsky</i>	0.225	1.024e-3	0.193	3.360e-4

5-Please update Fig. 12 by adding the noise content to the theoretical curve.

(5) For the rigor of the paper, according to your suggestion, Fig.3 in the manuscript has been updated as follows:

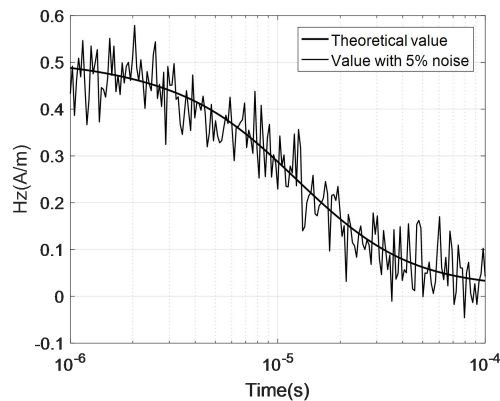


Fig.3 Forward data of Hz and data with 5% noise

6- How did you obtain error values less than the noise content added to the theoretical data?

(6) The relative error values in the paper are defined as follows, where the total relative error is the sum of the relative errors which of the resistivity and layer thickness parameters of the layered geoelectric model inversion, and the following is added to the '*3-layered H type model*' section of the manuscript:

The relative error is defined as

$$Err_{rel} = \left| \frac{T_{cal}^* - O_{ref}^*}{O_{ref}^*} \right| \quad (3)$$

where T_{cal}^* , O_{ref}^* are the calculated and reference value for the geoelectric models.

Furthermore, in order to verify the robust performance of the proposed algorithm, 5% and 10% noise are added to the theoretical data, and then inverted by the BP and COPSO-BP. Since the trained BP neural network can correctly predict for the trained mode or noisy mode, that is, BP neural network has the generalization ability to apply learning results to new knowledge. In addition, BP neural network does not have a great impact for global training results after its partial or partial neurons are destroyed, that is, BP neural network has a certain fault tolerance. Therefore, even for theoretical data with large noise, it can get better results by inversion, and then get the total relative error. Using the chaotic oscillation inertia particle swarm optimization algorithm (COPSO) with accelerated convergence to correct the initial parameters of BP that can avoid its local optimization, so that strengthening its generalization ability, fault tolerance and anti-noise performance. The relative error obtained inverting the noise-containing data by the COPSO-BP algorithm is smaller than these of the BP algorithm inversion, as shown in Table 2.

Table 2 Comparison of inversion results for three-layer H type (with noise) model

model parameters	resistivity $\rho(\Omega \cdot m)$			thickness h(m)		Total relative error(%)	
	ρ_1	ρ_2	ρ_3	h_1	h_2		
true value	100	10	100	100	200	--	
without noise	BP	99.724	9.937	100.765	99.031	198.701	3.284
	COPSO-BP	100.031	9.991	99.310	100.234	200.886	1.487
5% noise	BP	101.374	9.966	98.283	101.255	199.282	5.039
	COPSO-BP	100.252	9.977	98.222	101.206	199.228	3.847
10% noise	BP	90.525	9.931	99.481	101.748	203.105	13.976
	COPSO-BP	104.472	9.96050	101.345	100.570	199.437	7.064

7-Considering Fig. 14 that present the results of two approaches, the same resistivity range and contour interval must be used.

(7) Special thanks to your careful review. For the rigor of the article, we modified Fig.14 in the manuscript to use the same resistivity range and contour spacing as shown below.

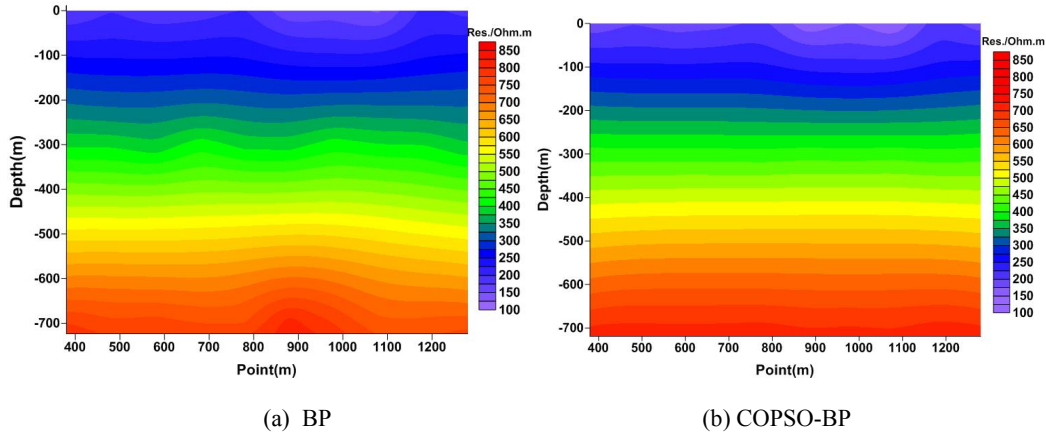


Fig. 4. Inversion results of BP (a) and COPSO-BP (b).

8-You should also mention in the paper which model parameters did you obtain through the PSO part of the algorithm at the end of 30 iterations. What are their error values as initial estimates requiring by the BP approach?

(8) In the research of this paper, because the BP neural network is very sensitive to the initial network weight, the network is initialized with different weights, which tends to converge to different local minimums, resulting in different results for each training. In view of the fact that the neural network is sensitive to the initial weight and easy to fall into the local minimum, the heuristic global search particle swarm optimization algorithm (PSO) with simple structure, fast convergence and high precision is used to optimize the initial weight and threshold of the neural network. That is, after 30 iterations of the PSO algorithm, the initial weights and thresholds of the BP neural network are obtained, and then the COPSO-BP is trained, so that the inversion parameters of the geoelectric model are not easy to fall into the local optimum, resulting in better model parameter results. In order to facilitate the reader's understanding, the 'BP Neural Network with COPSO algorithm' section in the manuscript supplements the following:

therefore, the COPSO algorithm is proposed to optimize the initial weight and threshold of BP.

For different research models, the initial estimation error of the BP method (the following formula 4) is usually different, and the BP neural network itself is a black box. It is difficult to confirm the initial estimation value, which is random, so the paper does not give a clear initial estimated error value. However, according to a large number of simulation experiments, the initial estimation mean square error(MSE) of the model parameters for the layered geoelectric model studied in this paper is within 1, as shown in Fig. 5.

The formula for calculating the i -th particle fitness is defined as

$$f_i = \frac{1}{S} \sum_{s=1}^S \sum_{j=1}^m (Y_{sj} - \hat{Y}_{sj})^2 \quad (4)$$

where S is the number of training set samples, m is the output neurons number, Y_{sj} is the j -th true output of the s -th sample, and \hat{Y}_{sj} is the corresponding predict output.

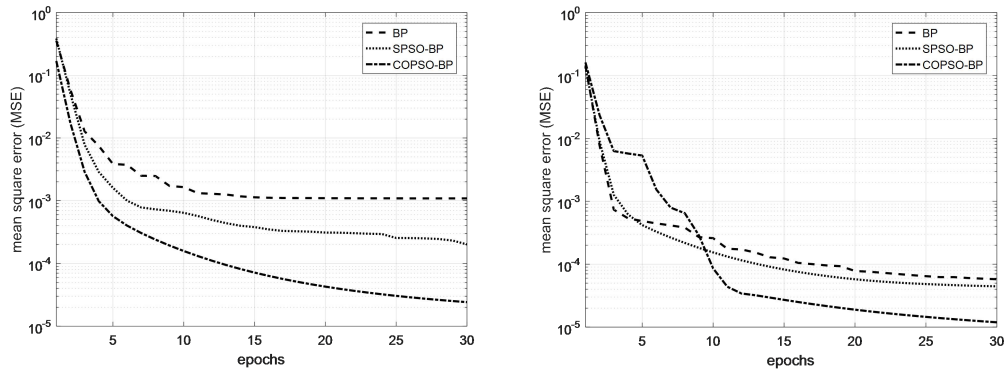


Fig. 5 Mean square error curves comparison for three-layer H type and five-layer KHK type geoelectric model

9-The title of the paper should be reconsidered by the authors. What does it mean “Transient Electromagnetic Inversion”. Think about “A fast approximation for 1D Inversion of Transient Electromagnetic Data by ..” or etc.

(9) Sincerely thank you for your comments. Compared with the title of the article in the previous manuscript, we agree that your comments on the title of the article are very pertinent and more suitable for the content of the study, so we modify the following based on your comments:

A fast approximation for 1D Inversion of Transient Electromagnetic Data by BP Neural Network and improved Particle Swarm Optimization.

Special thanks to you for your good comments.

Reviewer #2:

Dear reviewers:

Comments:

For final publication, the manuscript should be accepted as is.

Special thanks to you for your good support.

We tried our best to improve the manuscript and made some changes in the manuscript. These changes will not influence the content and framework of the paper. And here we did not list the changes but marked in red in revised paper.

We appreciate for Editors/Reviewers’ warm work earnestly, and hope that the correction will meet with approval.

Once again, thank you very much for your comments and suggestions.

A fast approximation for 1D Inversion of Transient Electromagnetic Data by BP Neural Network and improved Particle Swarm Optimization ~~BP Neural Network and improved Particle Swarm Optimization for Transient Electromagnetic Inversion~~

Ruiyou Li, Huaiqing Zhang*, Nian Yu, Ruiheng Li, Qiong Zhuang

The State Key Laboratory of Transmission Equipment and System Safety and Electrical New Technology, Chongqing University, Chongqing, 400044, China

1378546842@qq.com (Ruiyou Li); zhanghuaiqing@cqu.edu.cn (Huaiqing Zhang); 61408155@qq.com (Nian Yu); 392361773@qq.com (Ruiheng Li); 779695034@qq.com (Qiong Zhuang)

*Correspondence to: zhanghuaiqing@cqu.edu.cn

Abstract. As one of the most active nonlinear inversion methods in transient electromagnetic (TEM) inversion, the back propagation (BP) neural network has high efficiency because the complicated forward model calculation is unnecessary in iteration. The global optimization ability of the particle swarm optimization (PSO) is adopted for amending BP's sensitivity on initial parameters, which avoids it falling into local optimum. A chaotic oscillation inertia weight PSO (COPSO) is proposed in accelerating convergence. The COPSO-BP algorithm performance is validated by two typical testing functions, then by two geoelectric models inversion and a field example. The results show that the COPSO-BP method has better accuracy, stability and relative less training times. The proposed algorithm has a higher fitting degree for the data inversion, and it is feasible in geophysical inverse applications.

Keywords: transient electromagnetic inversion; BP neural network; particle swarm optimization; chaotic oscillation

1 Introduction

Transient electromagnetic (TEM) method applies the secondary receiving voltage induced by the rapid switching off pulse current, and then deduces the geo-electrical parameters consisting of the resistivities and thicknesses of the layers~~geoelectric structure parameters~~. The later is a typical TEM inversion issues with nonlinear feature. The linear inversion method was simple and widely used through linearization process, yet it is extremely dependent on initial parameters selection and resulting in poor inversion accuracy. Hence, the nonlinear inversion methods attract more geophysicists attention in recent years.

33 The artificial neural network(ANN) is one of the most active nonlinear inversion methods, it has
34 very high computation efficiency because the complicated forward model calculation is
35 unnecessary in iteration. All the ~~geoelectric parameters~~geolectrical parameters and the forward
36 model relations are implied in the weight and threshold parameters of ANN. And it is different
37 from the non-linear Monte Carlo method with global space search solution (He et al., 2018; Jha et
38 al., 2008; Pekşen et al., 2014; Sharma, 2012; Tran and Hiltunen, 2012). Srinivas et al. (2012)
39 compared the inversion performance of BP, radial basis function(RBF) and generalized regression
40 neural network (GRNN) in vertical electrical sounding data, then established a 1-D inversion
41 model with BP and finally realized the parameters inversion. Maiti et al. (2012) proposed a
42 Bayesian neural network training method in 1-D electrical sounding. Jiang et al. (2018) improved
43 the training method for kernel principal component wavelet neural network and achieved the
44 resistivity imaging. Jiang et al. (2016a) gave a learning algorithm based on information criterion
45 (IC) and particle swarm optimization for RBF network which improves the global search ability.
46 Johnson (2017) utilized neural network method to invert multi-layer georesistivity sounding. Jiang
47 et al. (2016b) presented a pruning Bayesian neural network (PBNN) method for resistivity
48 imaging and solved the instability, local minimization problems. Raj et al. (2014) solved
49 non-linear apparent resistivity inversion problems with ANN. The ANN has been widely applied
50 in electric prospecting data interpretation for its powerful fitting ability. However, the neural
51 network method is sensitive to initial parameter settings and falls easily into local minimum. Lots
52 improved methods were proposed for balancing the convergence rate and inversion quality. Zhang
53 and Liu (2011) proposed ant colony optimization for ANN and applied in high density resistivity,
54 acquired smaller inversion errors and higher determinant coefficients. Dai et al. (2014) suggested a
55 differential evolution (DE) for BP which enhanced the global search ability. Marina et al. (2014)
56 introduced the genetic algorithm for ANN.

57 The Particle swarm optimization (PSO) has simple structure, fast convergence rate, high
58 accuracy and global optimization ability. Fernández et al. (2010) successfully introduced the PSO
59 in 1-D resistivity inversion. Godio and Santilano (2018) applied it in geophysical inversion and
60 deduced a depth resistivity earth model. Since the PSO's global searching performance, the BP's
61 initial weights and thresholds can be trained by PSO and then the BP's global optimization ability
62 can be improved. Comparing to the standard PSO (SPSO), a chaotic oscillation inertia weight PSO
63 (COPSO) which can accelerate the convergence rate in the early stage was proposed naturally(Shi
64 et al., 2009).

65 The paper structure is as following: the principle of PSO algorithm with different inertia

Conflicts of Interests

The authors declare that they have no conflict of interest.

66 weights schemes, the BP neural network and the proposed COPSO-BP algorithm are given in
67 section 2. Then, the COPSO-BP algorithm performance is validated by two typical testing
68 functions in section 3. And in later section, inversion simulations of a three-layer and five-layer
69 geoelectric models are carried out, the hidden layer neuron numbers determining method is put
70 forward and algorithms performance is compared.

71 2 Principle of COPSO-BP Algorithms

72 2.1 Chaotic Oscillation PSO algorithm

73 For N -dimensional optimization problem, supposing the position (resistivity and thickness for
74 layered model parameters inversion) and velocity(update speed) of the i -th particle (global search
75 group number) at time t are $x_i = (x_{i1}, x_{i2}, \dots, x_{iN})$ and $v_i = (v_{i1}, v_{i2}, \dots, v_{iN})$ respectively. Then, at time
76 $t+1$, they can be calculated by the iterations as

$$77 \quad v_{id}^{t+1} = \omega \cdot v_{id}^t + c_1 r_1 (p_{id}^t - x_{id}^t) + c_2 r_2 (p_{gd}^t - x_{id}^t) \quad (1)$$

$$78 \quad x_{id}^{t+1} = x_{id}^t + v_{id}^{t+1} \quad (2)$$

79 where r_1, r_2 are random value evenly distributed in the interval (0,1), c_1, c_2 are learning factors
80 (usually equal to 2). And p_{id}, p_{gd} means the individual and global maximum.

81 The inertia weight parameter ω affects the algorithm performance seriously. A fixed weight
82 always was used in the early time, and then various dynamic weights were proposed. Shi et al.
83 (2010) have summarized several methods as

$$84 \quad \omega_1(t) = \omega_s - (\omega_s - \omega_e) t / T_{\max} \quad (3)$$

$$85 \quad \omega_2(t) = \omega_s - (\omega_s - \omega_e) (t / T_{\max})^2 \quad (4)$$

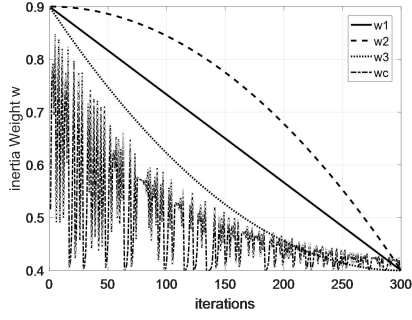
$$86 \quad \omega_3(t) = \omega_s - (\omega_s - \omega_e) [2t / T_{\max} - (t / T_{\max})^2] \quad (5)$$

87 Where ω_s and ω_e are the start and end weight. The t, T_{\max} are the current and maximum iteration.
88 The above weights are of smooth and monotonically decreasing. In this paper, we proposed a
89 decreasing oscillation weights scheme which was based on chaotic logistic equation. Its specific
90 calculation formula as

$$91 \quad x_{t+1} = \mu x_t (1 - x_t) \quad t = 0, 1, 2, \dots, n \quad (6)$$

$$92 \quad \omega_c(t) = \omega_e + (\omega_s - \omega_e) (0.99^t \cdot x_t) \quad (7)$$

93 where μ is the control parameter. A complete chaos state is established for $x \in (0,1)$ and $\mu = 4$, an
94 inertia weight is then obtained from Eq.(7). Numerical experiments were carried out
95 correspondingly and showed that the initial value of x_0 has little effect on inertia weight ω . The
96 inertia weights comparison was shown in Fig.1 where $x_0 = 0.234$ and $\mu = 4$ for chaotic oscillation.

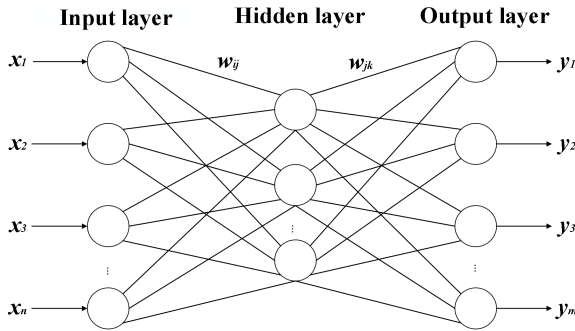


97

98 **Fig. 1** Inertial weight curves comparison

99 **2.2 BP Neural Network**

100 BP neural network is multi-layer feed forward structure, and a typical three-layer network is
 101 shown in Fig. 2 (Yong et al., 2009).



102

103 **Fig. 2** Three-layer BP neural network structure

104 where x_1, x_2, \dots, x_n are the input value, y_1, y_2, \dots, y_m are the predicted output, w_{ij}, w_{jk} are the network
 105 weights. The threshold parameter α is defined in hidden layer with its output

106
$$H_j = f\left(\sum_{i=1}^n w_{ij} x_i - \alpha_j\right) \quad j = 1, 2, \dots, l \quad (8)$$

107 where l is the hidden layer nodes numbers, f is the activation function with different expressions,
 108 and the most widely used is sigmoid type function. The predicted output for the k -th unit is
 109 calculated by

110
$$O_k = \sum_{j=1}^l H_j w_{jk} - b_k \quad (9)$$

111 And parameter b means the output threshold. Then the prediction error can be determined based
 112 on predicted output O_k and the expected output T_k as $e_k = (T_k - O_k)O_k(1 - O_k)$. The updating formula
 113 for weights and thresholds are as following

$$\left\{ \begin{array}{l}
w_{ij} = w_{ij} + \eta H_j (1 - H_j) x_i \sum_{k=1}^m w_{jk} e_k \\
w_{jk} = w_{jk} + \eta H_j e_k \\
\alpha_j = \alpha_j + \eta H_j (1 - H_j) \sum_{k=1}^m w_{jk} e_k \\
b_k = b_k + e_k
\end{array} \right. \quad (10)$$

115 where $i=1,2,\dots,n; j=1,2,\dots,l; k=1,2,\dots,m$; and η is the learning rate.

116 2.3 BP Neural Network with COPSO algorithm

117 The initial parameters are chosen randomly, which affects the convergence rate, learning
118 efficiency and perhaps falling into local minimum. The Chaotic Oscillation PSO (COPSO) has a
119 much better global optimization capability, therefore, the COPSO algorithm is proposed to optimize
120 the initial weight and threshold of BP~~we proposed the COPSO algorithm for BP parameters?~~
121 training. The COPSO-BP pseudo-codes were briefly described as following:

122
123 **Table.1** Pseudo-codes of COPSO-BP algorithm

-
- 1: *BP network structure definition* (neuron numbers n, l, m , and activation function)
 - 2: *COPSO initialization for BP* (weights, threshold as X . PSO parameters as $V_{\min}, V_{\max}, \omega, c_1, c_2$, size M , T_{\max})
 - 3: *Initializing BP* with X_i ($i=1, 2, \dots, M$) and *evaluating fitness* by Eq.(11) for each individual
 - 4: Setting the p_{id} and p_{gd}
 - 5: **While** $iter < T_{\max}$ **do**
 - 6: updating inertia weight by Eq.(7)
 - 7: **for** $i=1:M$ (all particles) **do**
 - 8: updating velocity V_i by Eq.(1)
 - 9: updating particle position X_i by Eq.(2)
 - 10: *Initializing BP* with new X_i and *calculating fitness* by Eq.(11)
 - 11: **if** X_i is better than p_{id}
 - 12: Set X_i is to be p_{id}
 - 13: **End if**
 - 14: **if** X_i is better than p_{gd}
 - 15: Set X_i is to be p_{gd}
 - 16: **End if**
 - 17: **End for** i
 - 18: $iter = iter + 1$
 - 19: **End While**
 - 20: *Initializing BP* with p_{gd}
 - 21: *Inputting and obtaining the predicted output*
-

124 The formula for calculating the i -th particle fitness is defined as

$$f_i = \frac{1}{S} \sum_{s=1}^S \sum_{j=1}^m (Y_{sj} - \hat{Y}_{sj})^2 \quad (11)$$

where S is the number of training set samples, m is the output neurons number, Y_{sj} is the j -th true output of the s -th sample, and \hat{Y}_{sj} is the corresponding predict output.

3 Algorithm Testing

In order to investigate the COPSO-BP performance and reliability, Rosenbrock and Bohachevsky testing functions were adopted, which are typical non-convex functions and mainly to evaluate the performance of unconstrained algorithms. However, due to the random nature of the function, it is not easy to solve and has a global minimum function value of zero.

~~In order to investigate the COPSO-BP performance and reliability, two typical testing functions were adopted and simulations were performed in MATLAB.~~

(1) *Rosenbrock* function:

$$f_1(x) = 100 \times (x_1^2 - x_2)^2 + (1 - x_1)^2, x_i \in [-10, 10], i = 1, 2 \quad (12)$$

(2) *Bohachevsky* function:

$$f_2(x) = x_1^2 + x_2^3 - x_1 x_2 x_3 + x_3 - \sin(x_2^2) - \cos(x_1 x_3^2), x_i \in [-2\pi, 2\pi], i = 1, 2, 3 \quad (13)$$

The standard PSO-BP (SPSO-BP) with linear decreasing inertia weight as Eq.(3), the COPSO-BP were carried out respectively. The three-layer BP of n - s -1 structure is constructed with different hidden nodes. The PSO parameters are population size $M = 60$, learning factors $c_1 = c_2 = 2.0$, the maximum iteration $T_{\max} = 30$, inertia weight $\omega_s = 0.9$, $\omega_e = 0.4$, $x_0 = 0.234$ and $\mu = 4$ for chaotic parameters, the search dimension $D = n \times s + s \times 1 + s + 1$ which includes all the neuron weights and thresholds. For BP network, 150 training samples and 50 testing samples were randomly produced within the variable range. The training error is defined as

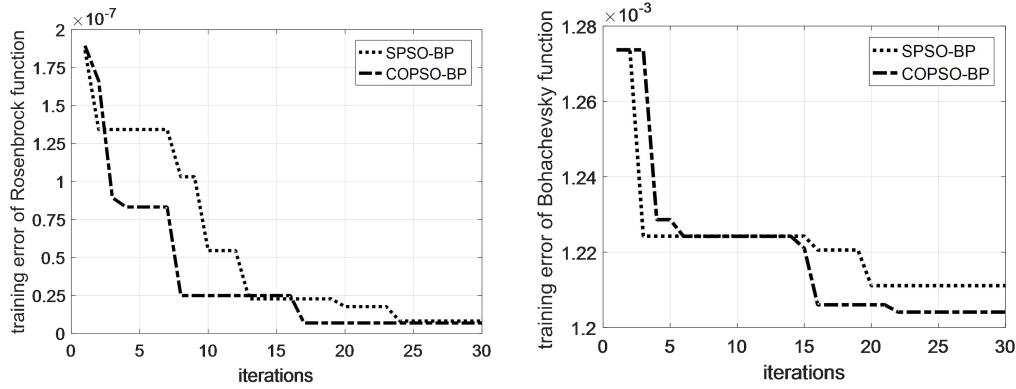
$$E = \frac{1}{S} \sum_s (T_s - O_s)^2 \quad (14)$$

where S is the training samples number, T_s , O_s are the expected and predicted output for training sample s respectively. The network structures with minimum training errors for *Rosenbrock* and *Bohachevsky* functions are 2-7-1 and 3-6-1 respectively. The simulation performs 20 times for each testing function with SPSO-BP and COPSO-BP algorithms. The numerical result was shown in Table.2. One of the evolutionary training error curves (select one in 20 times randomly) were shown in Fig.3, and the fitting curves of COPSO-BP algorithm were shown in Fig.4.

Table.2 Comparison of SPSO-BP and COPSO-BP algorithm for testing functions

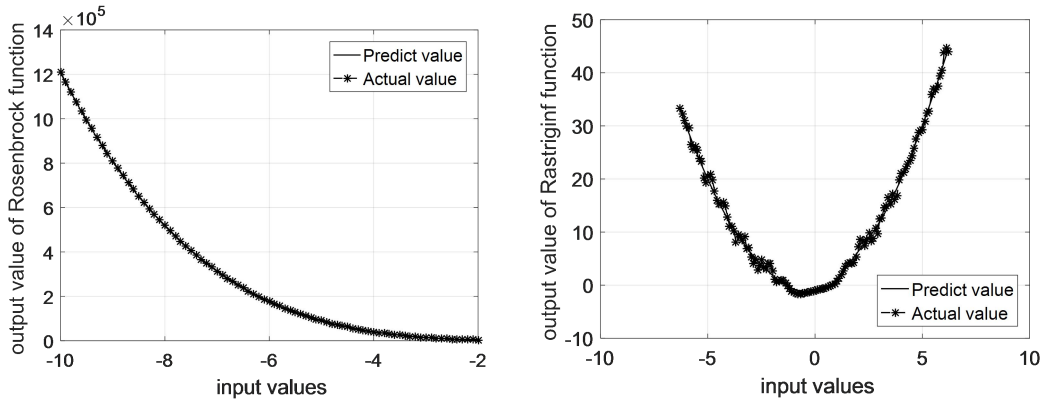
Testing functions	SPSO-BP		COPSO-BP	
	Average value	Optimal value	Average value	Optimal value

<i>Rosenbrock</i>	2.375e-3	2.300e-5	1.201e-3	2.410e-06
<i>Bohachevsky</i>	0.225	1.024e-3	0.193	3.360e-4



154
155

Fig. 3 Training error curves of SPSO-BP and COPSO-BP algorithms



156

Fig. 4 Fitting curves of COPSO-BP algorithm

157

158

It can be seen in Table.2 that both the SPSO-BP and COPSO-BP algorithms can acquire a relative high accuracy for testing functions, the COPSO-BP is a slightly better than SPSO-BP. However, the COPSO-BP has better convergence rate and optimization efficiency in the early stage in Fig.3. Therefore, the SPSO-BP and COPSO-BP algorithms have strong learning ability, good stability and generalization ability, which will be suitable for TEM inversion.

159

160

161

162

163

4 Layered model and parameter analysis

164

4.1 Forward Model

165

According to Kaufman's derivation (1983), the frequency response of central loop source for the layered model takes the following Hankel transform

166

167

$$H_z(\rho, \omega) = Ia \int_0^{\infty} \frac{m^2}{m + m_1/R_1^*} J_1(m\rho) dm \quad (15)$$

168

169

170

171

172

where a is the radius of transmitting coil, I is the excitation current, ρ is the center distance between the transmitting coil and the receiving coil, $J_1(m\rho)$ is the first-order Bessel function, m is integral variable, $m_1 = (m^2 - k_1^2)^{1/2}$, k_1 is the conduction current, σ_1 is the conductivity, $k_1 = -i\omega\mu\sigma_1$, and R_1^* is the first layer apparent resistivity conversion function which can be obtained by the following recurrence formula

$$173 \quad \begin{cases} R_n^* = 1 \\ R_j^* = \frac{m_j R_{j+1}^* + m_{j+1} \text{th}(m_j h_j)}{m_{j+1} + m_j R_{j+1}^* \text{th}(m_j h_j)} \end{cases} \quad (16)$$

174 There is no analytical solution for the time-domain response for layered model, it can only be
 175 solved by numerical calculation. The Hankel transform in formula (15) is calculated by an
 176 improved digital filtering algorithm with 47 points J_1 filter coefficient, and then time response can
 177 be obtained using the Gaver-Stehfest transform as follows:

$$178 \quad H_z(\rho, t) = \frac{\ln 2}{t} \sum_{n=1}^N K_n H_z(\rho, s_n) \quad (17)$$

179 where $s_n = (\ln 2/t) \times n$, K_n is the coefficient, N is determined by the computer bits, generally N=12.

180 The ramp excitation current of TEM is

$$181 \quad I(t) = \begin{cases} 0, & t < 0 \\ t/T_1, & 0 \leq t < T_1 \\ 1, & T_1 < t \end{cases} \quad (18)$$

182 where T_1 is the turn-off time, and the Laplace transform is

$$183 \quad I(s) = \frac{1}{T_1 s^2} - \frac{1}{T_1 s^2} e^{-T_1 s} = \frac{1}{T_1 s^2} (1 - e^{-T_1 s}) \quad (19)$$

184 Therefore, for a specific layered model, the apparent resistivity conversion function R_1^* is firstly
 185 calculated by recurrence formula (16) based on geoelectric structure parameters. And then the
 186 frequency response at fixed point $H_z(\omega)$ is calculated by Hankel transform as formula (15). For
 187 ramp excitation, the Laplace transform of $H_z(s)$ should multiplied by $I(s)$. Finally, the time
 188 response $H_z(t)$ is obtained by Gaver-Stehfest transform as formula (17). So the $H_z(t)$ is obtained by
 189 a Gaver-Stehfest transform, a Hankel transform and a recurrence calculation, and it is somewhat
 190 heavy computational consuming.

191 However, the vertical magnetic field $H_z(t)$ is the actual observed signal in transient
 192 electromagnetic method in engineering applications. It is the inversion input and output is
 193 geoelectric structure parameters. A method which can avoid the complicated forward model
 194 calculation is of great importance in algorithm efficiency.

195 4.2 BP network design and COPSO algorithm

196 For BP structure, the output nodes are determined by the number of inversion ~~geoelectric-~~
 197 ~~parameters~~geoelectrical parameters, the input nodes are determined by the samples number of
 198 $H_z(t)$, the hidden nodes varies according to approximation performance. As a three-layer or
 199 five-layer geoelectric model, its ~~geoelectric-parameters~~geoelectrical parameters are 5 (three
 200 resistivity and two thickness parameters) or 9 (five resistivity and four thickness parameters), the
 201 output nodes are 5 or 9 correspondingly. The characteristic samplings of $H_z(t)$ are chosen as 10 or

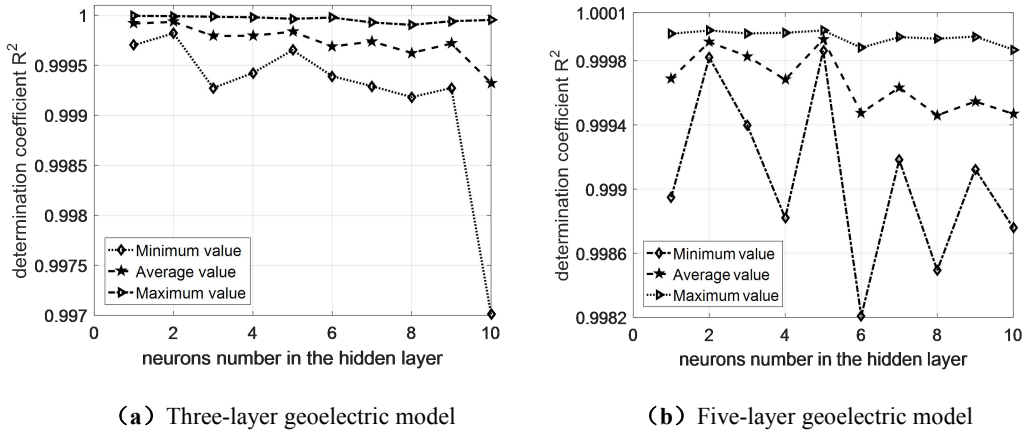
202
203
204
205
206

20, which are determined by the model's complexity, more layers mean more sampling points needed. The 10 samplings were selected in this paper hence with 10 input nodes. While for the hidden layer neuron, its number is related to the weights and threshold parameters amount directly and affects the BP performance greatly. An appropriate hidden nodes number is necessary and a determination coefficient R^2 is defined for evaluating as

$$R^2 = \frac{\left(n \sum_{i=1}^n Y_i \hat{Y}_i - \sum_{i=1}^n Y_i \sum_{i=1}^n \hat{Y}_i \right)^2}{\left(n \sum_{i=1}^n \hat{Y}_i^2 - \left(\sum_{i=1}^n \hat{Y}_i \right)^2 \right) \left(n \sum_{i=1}^n Y_i^2 - \left(\sum_{i=1}^n Y_i \right)^2 \right)} \quad (20)$$

208
209
210
211
212
213
214

where Y_i is the true value, \hat{Y}_i is the predicted value for i -th training data, n is the training data number. A larger determination coefficient means a better approximation performance. The simulations on hidden nodes effect were carried out for a three-layer and five-layer geoelectric models. The BP structure is 10- s -5 and 10- s -9, its transfer, training and learning functions are 'Log sigmodial', 'Levenberg-Marquardt' and 'Gradient descent momentum' respectively. The average, minimum and maximum value of R^2 were obtained after running 20 times for each simulation. The R^2 curves were shown in Fig.5.



215
216
217
218
219
220
221
222

Fig. 5 Influence of hidden layer nodes on R^2 for different geoelectric model

It can be seen that the optimal neural network structures were 10-2-5 and 10-5-9 for three and five-layer models based on the maximum R^2 . Then, the PSO-BP algorithms with different inertia weight were implemented and compared for three-layer model. The BP structure was chosen as 10-2-5, four types of inertia weight as Eq. (3~7) in PSO were compared in Table.3.

Table.3 Comparison of different inertia weights in PSO algorithms ($\omega_s = 0.9, \omega_e = 0.4$)

inertia weight	iteration number	minimum fitness	average fitness	convergence time(s)
ω_1	9	1.3914e-3	1.3982e-3	65.21
ω_2	29	1.4406e-3	1.4418e-3	204.97
ω_3	25	1.4168e-3	1.4224e-3	189.17

223 The simulation was implemented on Core (TM) i5-7500 with 8GB memory. It is obviously
 224 found in Table.3 that the COPSO algorithm has much faster convergence rate, less iteration
 225 number and time consuming.

226 4.3 Layered model inversion

227 A 3-layered and 5-layered geoelectric models were investigated, which the PSO parameter values
 228 are the same as those of the Algorithm Testing parts in the paper. In order to simulate actual TEM
 229 applications, the ramp turn-off is taken into account. Considering the probability distribution
 230 characteristic of above algorithms, the average of 20 simulation results is chosen. The BP,
 231 SPSO-BP, COPSO-BP algorithms and non-linear programming genetic algorithm (NPGA) (Li et
 232 al., 2017) were compared.

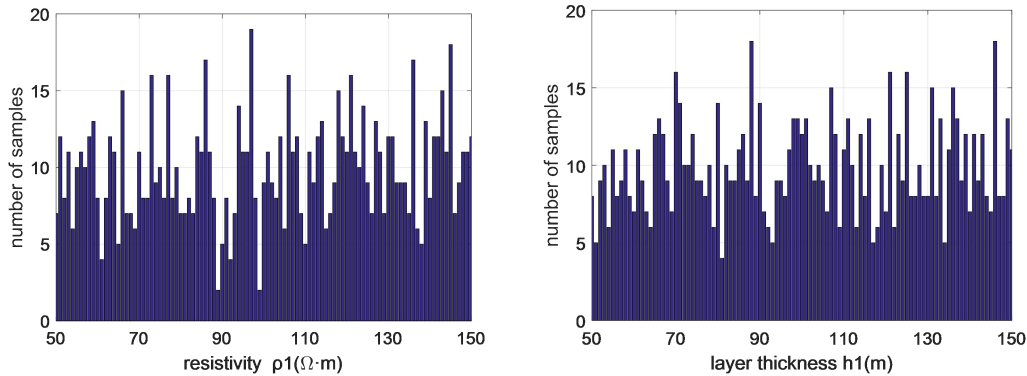
233 (1) 3-layered H type model

234 The central loop TEM parameters are set as following, transmitting coil radius $a = 100$ m, ramp
 235 emission current is 100 A, turn-off time is 1 μ s. In the geoelectric model, the resistivity $\rho_1 = 100$
 236 $\Omega \cdot m$, $\rho_2 = 10 \Omega \cdot m$, $\rho_3 = 100 \Omega \cdot m$ and thickness $h_1 = 100$ m, $h_2 = 200$ m.

237 The BP training samples which is a series of $H_z(t)$ for different **geoelectric-**
 238 **parameters****geoelectrical parameters** were generated by TEM forward model. The resistivity ranges
 239 were $\rho_1 \in (50,150)$, $\rho_2 \in (5,15)$, $\rho_3 \in (50,150)$, the thickness range were $h_1 \in (50,150)$,
 240 $h_2 \in (100,300)$, and choosing 1000 random groups. The resistivity and thickness distributions of ρ_1
 241 and h_1 were shown in Fig.6. **The relative error is defined as**

$$242 \text{Err}_{rel} = \frac{|T_{cal}^* - O_{ref}^*|}{O_{ref}^*} \quad (21)$$

243 **where T_{cal}^* , O_{ref}^* are the calculated and reference value for the geoelectric models.**



244
 245 **Fig. 6** Distribution of resistivity ρ_1 and thickness h_1 in training samples

246 The inversion results were shown in Table.4. and Fig.7~8. The BP type algorithms were
 247 superior to the NPGA inversion in Table.4. Moreover, the inversion accuracy, convergence rate
 248 and optimization ability of the COPSO-BP algorithm were better than others.

Table.4 Inversion comparison of three-layer H type geoelectric model

H type	resistivity ρ ($\Omega \cdot m$)			thickness $h(m)$		total relative error(%)
	ρ_1	ρ_2	ρ_3	h_1	h_2	
true values	100	10	100	100	200	--
BP relative error(%)	-0.275	-0.625	0.765	-0.968	-0.649	3.284
SPSO-BP relative error(%)	0.062	-0.322	-0.737	-0.579	-0.970	2.672
COPSO-BP	100.031	9.991	99.310	100.234	200.886	--
COPSO-BP relative error(%)	0.031	-0.087	-0.689	0.234	0.443	1.487
NPGA relative error(%)	0.133	-0.034	3.450	-7.305	-0.401	11.323

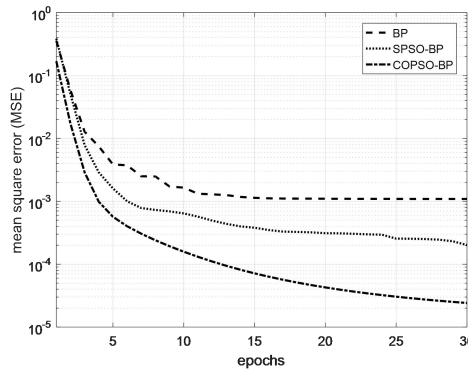
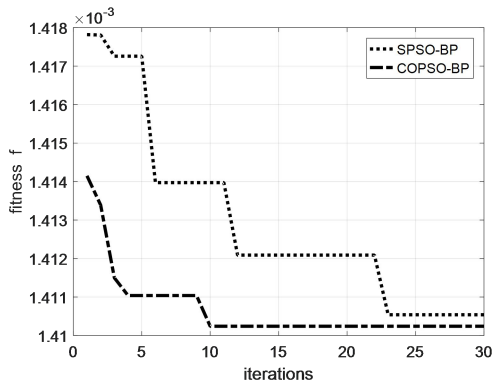


Fig. 7 Fitness curves of SPSO-BP and COPSO-BP **Fig. 8** Mean square error curves comparison

Additional results showed that the solution range of ρ_1 and h_1 in 20 times simulations for above algorithms were $\rho_1 \in (97.980, 103.102)$, $h_1 \in (96.962, 102.480)$ for BP, $\rho_1 \in (98.954, 101.137)$, $h_1 \in (96.955, 101.829)$ for SPSO-BP, $\rho_1 \in (99.382, 100.989)$, $h_1 \in (97.877, 101.044)$ for COPSO-BP respectively. Therefore, the COPSO-BP can acquire higher accuracy and is more stable.

(2) 5-layered KHK type model

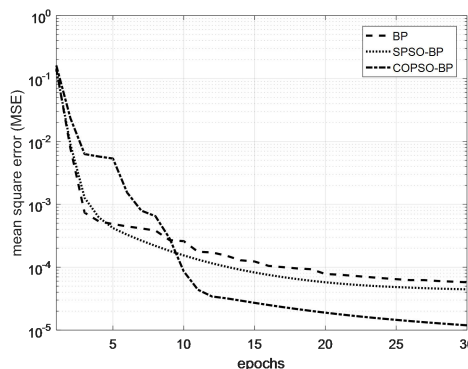
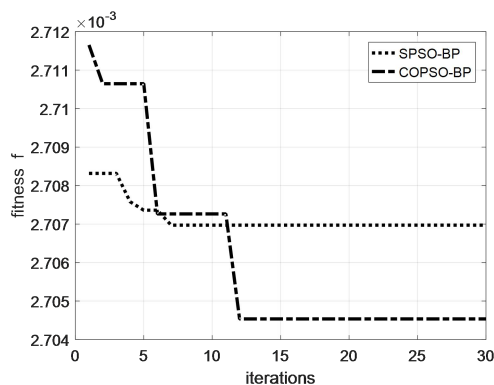
A 5-layered KHK type geoelectric model was adopted and its resistivity were $\rho_1 = 100 \Omega \cdot m$, $\rho_2 = 300 \Omega \cdot m$, $\rho_3 = 50 \Omega \cdot m$, $\rho_4 = 200 \Omega \cdot m$, $\rho_5 = 30 \Omega \cdot m$ and thickness were $h_1 = 100 m$, $h_2 = 200 m$, $h_3 = 300 m$, $h_4 = 500 m$.

The training samples with parameter ranges were $\rho_1 \in (50, 150)$, $\rho_2 \in (150, 450)$, $\rho_3 \in (25, 75)$, $\rho_4 \in (100, 300)$, $\rho_5 \in (15, 45)$ for resistivity, and $h_1 \in (50, 150)$, $h_2 \in (100, 300)$, $h_3 \in (150, 450)$, $h_4 \in (250, 750)$ for thickness. The 1000 groups training samples were generated within above ranges. The inversion results were shown in Table.5 and Fig.9~10. As can be seen that the COPSO-BP algorithm has better global optimization performance.

Table.5 Inversion comparison for five-layer KHK type geoelectric model

KHK type	resistivity $\rho(\Omega \cdot m)$					thickness $h(m)$				Total relative error(%)
	ρ_1	ρ_2	ρ_3	ρ_4	ρ_5	h_1	h_2	h_3	h_4	

true values	100	300	50	200	30	100	200	300	500	--
BP relative error(%)	-1.006	-0.862	-1.014	-0.030	1.119	-0.362	-0.298	-0.575	-0.376	5.645
SPSO-BP relative error(%)	0.429	1.040	-0.577	-0.071	-0.883	-0.002	0.657	-0.655	-0.316	4.634
COPSO-BP	99.594	299.469	50.082	199.092	29.937	99.501	200.481	301.800	497.670	--
COPSO-BP relative error(%)	-0.405	-0.176	0.164	-0.453	-0.209	-0.498	0.240	0.600	-0.465	3.214
NPGA relative error(%)	-6.211	-0.008	-0.974	3.930	3.083	-0.691	0.505	-2.900	-3.370	19.062



266

267 **Fig. 9** Fitness curves of SPSO-BP and COPSO-BP

Fig. 10 Mean square error curves comparison

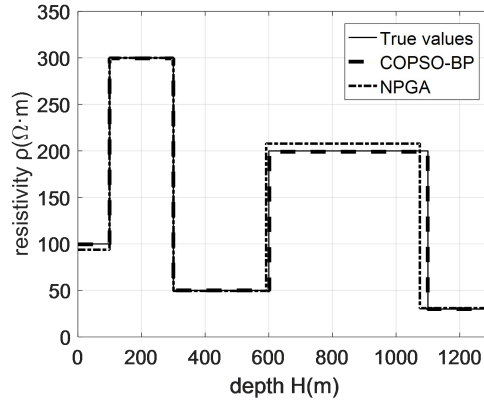
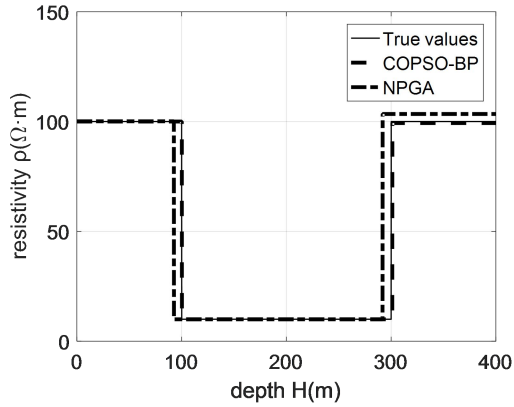
268 **(3) Inversion comparison**

269 Three kinds of BP methods as traditional BP, the SPSO-BP and the COPSO-BP algorithms were
 270 compared in Table.6. Hence, the training times of COPSO-BP was obviously less than SPSO-BP
 271 and was almost equal to BP, it can obtain better precision especially for its global optimization
 272 performance.

273 **Table.6** Simulation comparison for different algorithms

inversion method	three-layer H type model			five-layer KHK type model		
	training times	minimum training error	test relative error rate(%)	training times	minimum training error	test relative error rate(%)
BP	3	0.2882	3.284	5	0.3013	5.645
SPSO-BP	7	0.2832	2.672	15	0.2992	4.634
COPSO-BP	5	0.2725	1.487	6	0.2900	3.214

274 The inversion of COPSO-BP and NPGA were compared in Fig.11. The fitting ability of
 275 COPSO-BP was much better than NPGA.



(a) Three-layer H type geoelectric model

(b) Five-layer KHK type geoelectric model

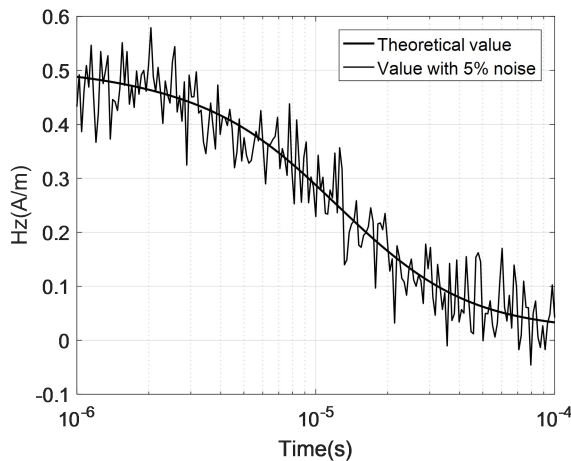
Fig. 11 Inversion comparison for different geoelectric models

(4) Robust performance analysis

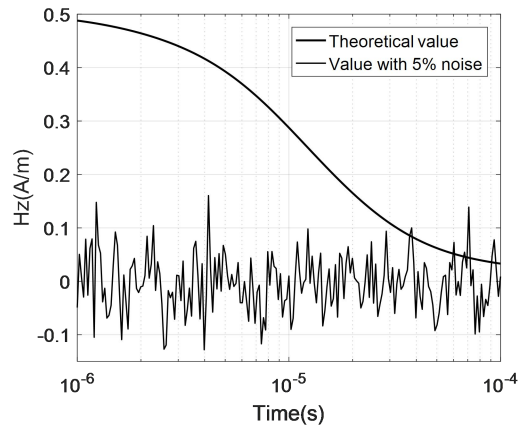
In order to verify the algorithm robustness, 5%(26dB) and 10%(20dB) Gaussian random noise was added in TEM data for three-layer geoelectric model. Three kinds of inversions were implemented respectively. The results and comparison were shown in Table.7. The $H_z(t)$ and data with 5% noise were shown in Fig.12.

Table 7 Comparison of inversion results for three-layer H type (with noise) model

model parameters	resistivity $\rho(\Omega \cdot m)$			thickness $h(m)$		Total relative error(%)	
	ρ_1	ρ_2	ρ_3	h_1	h_2		
true value	100	10	100	100	200	--	
without noise	BP	99.724	9.937	100.765	99.031	198.701	3.284
	COPSO-BP	100.031	9.991	99.310	100.234	200.886	1.487
5% noise	BP	101.374	9.966	98.283	101.255	199.282	5.039
	COPSO-BP	100.252	9.977	98.222	101.206	199.228	3.847
10% noise	BP	90.525	9.931	99.481	101.748	203.105	13.976
	COPSO-BP	104.472	9.96050	101.345	100.570	199.437	7.064



285



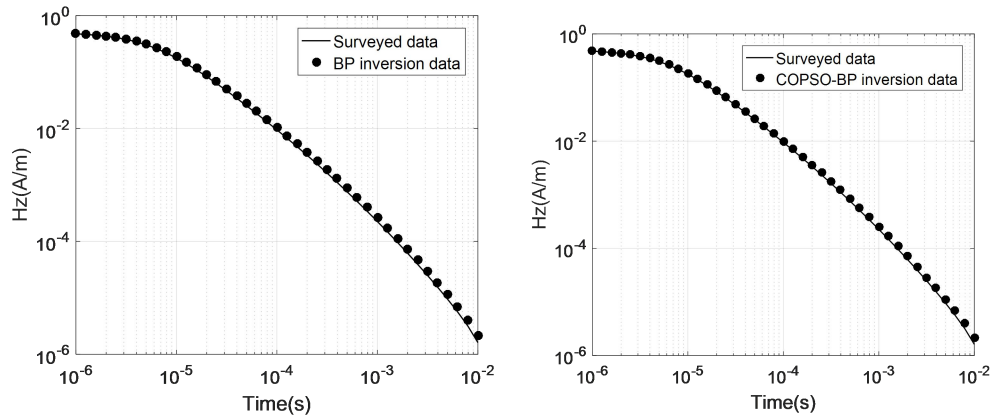
286

287 **Fig.12** Forward data of Hz and data with 5% noise

288 As can be seen from Table 3, after applying 5% and 10% Gaussian noise the COPSO-BP
 289 inversion has higher robust ability. The accuracy was obviously improved based on the total
 290 relative error data.

291 **4.4 Field example**

292 In order to test the effectiveness of the method, a transient electromagnetic vertical magnetic field
 293 (Hz) with 10 measuring points at the 380m to 1280m of the No. 1 line from a mining area in
 294 Anhui Province was selected. After the data processing, the inversion was performed using the
 295 3-layer neural network model in the previous section, and the results of BP and COPSOBP
 296 inversion were compared. Figure 13 shows the comparison between the surveyed data and the
 297 inversion data at 380m of the No. 2 line in the mining area. Figure 14 displays the pseudo-sections
 298 of the 10 sets of inversion data combined with the geological data interpolation smoothing. It can
 299 be seen from Fig. 14 that the first layer is a low resistivity (100~200 $\Omega \cdot m$), which is inferred to be
 300 the second layer (T2g22) gray dolomite of the Middle Triassic old Malague section, with a
 301 thickness of about 200 m; the second layer is the second highest resistivity (300~400 $\Omega \cdot m$), which
 302 is surmised to be the first layer (T2g21) dolomite of the Middle Triassic old Malaga section, with a
 303 thickness of about 400m; the third layer is high resistivity (600~800 $\Omega \cdot m$), which is speculated to
 304 be the 6th layer (T2g16) limestone dolomite of the Middle Triassic old group. The results are
 305 basically consistent with the geological conditions of the mining area, indicating the feasibility
 306 and effectiveness of the neural network method. And the results of COPSO-BP inversion are better
 307 than those of BP, which the inversion position is more accurate, the shape and spacing are clearer,
 308 and the resistivity of each layer is more consistent with the those of the actual geological model.



309

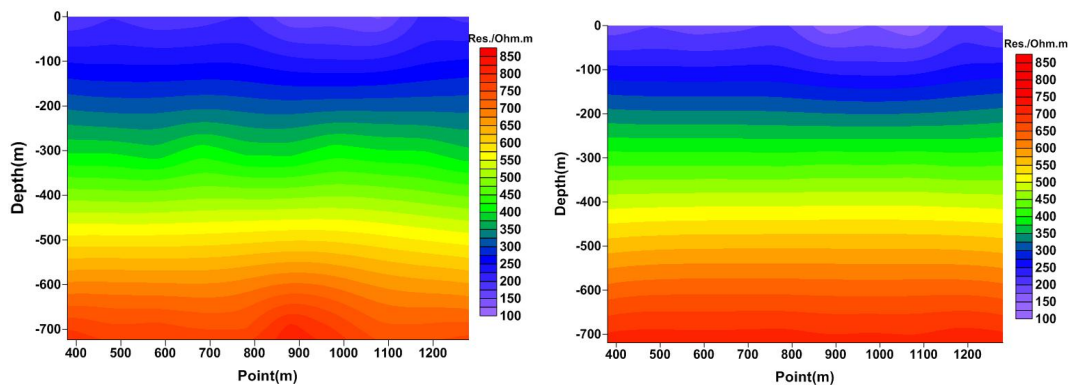
(a) BP

(b) COPSOBP

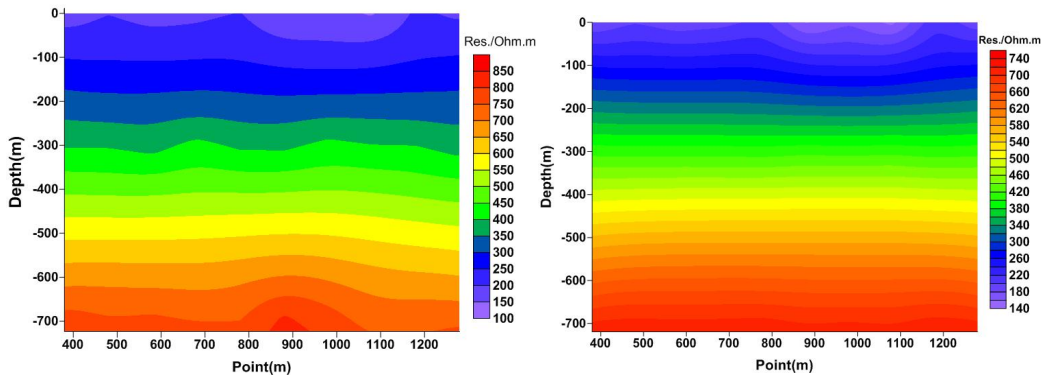
310

311

Figure 13. 1D inversion forward results. (a) BP; (b) COPSOBP.



312



313

(a) BP

(b) COPSO-BP

314

315

Figure 14. Inversion results of BP (a) and COPSO-BP (b).

316

5 Discussion

317

The inversion is performed for 3-layered (H-type) and 5-layered (KHK-type) geoelectric models

318

in this paper. The results show that the BP neural network is better than the NPGA algorithm,

319

because the BP method does not need to use the forward algorithm repeatedly, and its calculation

320

time is short, which is different from the nonlinear heuristic method based on global space search

321 solution.

322 The BP main advantage is that it can interpret the transient electromagnetic sounding results
323 quickly after training the network. Furthermore, BP algorithm could automatically obtain the
324 "reasonable rules" between input and output data by learning, and it can adaptively store the
325 learning content in the network weight, which the BP neural network has the high self-learning
326 and self-adaptation ability. In addition, the superior simulation results of the test function indicate
327 that the BP algorithm can approximate any nonlinear continuous function with arbitrary precision,
328 which means it has strong nonlinear mapping ability; the inversion results of the layered
329 geoelectric model with uncorrelated noise data prove that the BP algorithm has strong robustness,
330 which means it has the ability to apply learning results to new knowledge. However, the BP neural
331 network weight is gradually adjusted by the direction of local improvement, which causes the
332 algorithm to fall into local extremum, and the weight converges to a local minimum that leads to
333 the network training failure; Moreover, BP is very sensitive to the initial network weight, and the
334 initialization network with different weight values tends to converge to different local minimums,
335 so that obtains different results each time; In addition, the BP algorithm is a gradient descent
336 method essentially, which leads to a slow convergence rate.

337 From the results of the layered model and parametric analysis part, it can be seen that single
338 BP algorithm has higher error value than SPSO-BP, because BP method is sensitive to initial
339 weight and easy to fall into local minimum values, thus a heuristic global search particle swarm
340 optimization algorithm with simple structure, rapid convergence and high precision is applied to
341 optimize the weight and threshold of BP neural network, which improves the global optimization
342 performance of the algorithm. Furthermore, the PSO algorithm adjusts the inertia weight
343 adaptively based on the chaotic oscillation curve that is similar to the annealing process in the
344 simulated annealing algorithm (SA), which jumps out the local extremum faster in the early stage
345 and accelerates the convergence and reduces the training times. Therefore, compared with
346 SPSO-BP and BP algorithm, the inversion results of COPSO-BP are closer to the theoretical data
347 with smaller error fluctuations, stronger anti-noise, better generalization performance and higher
348 stability, which it is effective in solving geophysical inverse problems.

349 From the simulation experiment, it is not clear how the weight organization affects the BP
350 neural network weight learning process. It is necessary to conduct a more systematic study on this
351 problem to improve our understanding of how BP neural network handles training data.

352 **6 Conclusion**

353 The nonlinear COPSO-BP method was proposed for TEM inversion. The BP's initial weight and
354 threshold parameters were trained by COPSO algorithm which makes it not easy to fall into local
355 optimum. The chaotic oscillation inertia weight for PSO was proposed so as to improve the PSO's
356 global optimization ability and fast convergence in early stage. The layered geoelectric model

357 inversion showed that the COPSO-BP method has better accuracy, stability and relative less
358 training times.

359

360 **Author Contributions**

361 Huaqing Zhang conceived this manuscript. Huaqing Zhang and Ruiyou Li developed the main
362 algorithmic idea and mathematical part. Ruiheng Li and Nian Yu carried out the simulation and
363 data analysis. Qiong Zhuang completed the writing and interpretation of this manuscript. All
364 authors contributed to the manuscript writing and approved the final manuscript.

365

366 **Competing interests**

367 The authors declare that they have no conflict of interest.

368

369 **Acknowledgments**

370 This work was partly supported by the National Natural Science Foundation of China
371 (No.51377174, No.51577016, No.51877014), the Fundamental Research Funds for the Central
372 Universities(No.2018CDQYDQ0005).

373 **Computer Code Availability**

374 Code name is PSOBP, developer is Huaqing Zhang and Ruiyou Li, contact address is
375 Chongqing University in China, telephone number is 13752954568 and e-mail is
376 zhanghuaqing@cqu.edu.cn, year first available, hardware required is a computer, software
377 required is MATLAB R2016a, program language is C++, program size is 10KB, and source code
378 from <https://github.com/liruiyou/PSOBP>.

379 **Reference**

380 Dai, Q., Jiang, F., and Dong, L.: Nonlinear inversion for electrical resistivity tomography based on chaotic DE-BP
381 algorithm, *J. Cent. South. Univ.*, 21, 2018-2025, <https://doi.org/10.1007/s11771-014-2151-9>, 2014.

382 Fernández Martínez, J. L., García Gonzalo, E., Fernández Álvarez, J. P., Kuzma, H. A., and Menéndez Pérez, C. O.:
383 PSO: A powerful algorithm to solve geophysical inverse problems: Application to a 1D-DC resistivity case,
384 *Journal of Applied Geophysics*, 71, 13-25, <https://doi.org/10.1016/j.jappgeo.2010.02.001>, 2010.

385 Godio, A., and Santilano, A.: On the optimization of electromagnetic geophysical data: Application of the PSO
386 algorithm, *Journal of Applied Geophysics*, 148, 163-174, <https://doi.org/10.1016/j.jappgeo.2017.11.016>, 2018.

387 Wang, H., Liu M. L., Xi, Z. Z., Peng, X. L., He, H.: Magnetotelluric inversion based on BP neural network
388 optimized by genetic algorithm, *Chinese Journal of Geophysics*, 61, 1563-1575 <https://doi.org/10.6038/cjg>
389 2018L0064, 2018.

390 Jha, M. K., Kumar, S., and Chowdhury, A.: Vertical electrical sounding survey and resistivity inversion using
391 genetic algorithm optimization technique, *J. Hydrol.*, 359, 71-87, <https://doi.org/10.1016/j.jhydrol.2008.06.018>,

392 2008.

393 Jiang, F., Dai, Q., and Dong, L.: An ICPSO-RBFNN nonlinear inversion for electrical resistivity imaging, *J. Cent.*
394 *South. Univ.*, 23, 2129-2138, <https://doi.org/10.1007/s11771-016-3269-8>, 2016a.

395 Jiang, F., Dai, Q., and Dong, L.: Nonlinear inversion of electrical resistivity imaging using pruning Bayesian
396 neural networks, *Journal of Applied Geophysics*, 13, 267-278, <https://doi.org/10.1007/s11770-016-0561-1>,
397 2016b.

398 Jiang, F., Dong, L., and Dai, Q.: Electrical resistivity imaging inversion: An ISFLA trained kernel principal
399 component wavelet neural network approach, *Neural Networks.*, 104, 114-123, <https://doi.org/10.1016/j.neunet>.
400 2018.04.012, 2018.

401 Kaufman, A. A., and Keller, G. V.: *Frequency and Transient Sounding*, Elsevier Methods in Geochemistry &
402 Geophysics, 1983.

403 Johnson, O. L., Aizebeokhai, A. P.: Application of Artificial Neural Network for the Inversion of Electrical
404 Resistivity Data, *Journal of Informatics and Mathematical Sciences*, 9, 297-316, 2017.

405 Li, F. P., Yang, H. Y., and Liu, X. H.: Nonlinear programming genetic algorithm in transient electromagnetic
406 inversion, *Geophysical and Geochemical Exploration*, 41, 347-353, 2017.

407 Maiti, S., Erram, V. C., Gupta, G., and Tiwari, R. K.: ANN based inversion of DC resistivity data for groundwater
408 exploration in hard rock terrain of western Maharashtra (India), *J. Hydrol.*, 464, 294-308,
409 <https://doi.org/10.1016/j.jhydrol.2012.07.020>, 2012.

410 Pekşen, E., Yas, T., and Kıyak, A.: 1-D DC Resistivity Modeling and Interpretation in Anisotropic Media Using
411 Particle Swarm Optimization, *Pure. Appl. Geophys.*, 171, 2371-2389,
412 <https://doi.org/10.1007/s00024-014-0802-2>, 2014.

413 Raj, A. S., Srinivas, Y. , and Oliver, D. H.: A novel and generalized approach in the inversion of geoelectrical
414 resistivity data using Artificial Neural Networks (ANN), *J. Earth Syst. Sci.*, 123, 395-411,
415 <https://doi.org/10.1007/s12040-014-0402-7>, 2014.

416 Rosas-Carbajal, M., Linde, N., Kalscheuer, T., and Vrugt, J. A.: Two-dimensional probabilistic inversion of
417 plane-wave electromagnetic data: methodology, model constraints and joint inversion with electrical resistivity
418 data, *Geophys. J. Int.*, 196, 1508-1524, <https://doi.org/10.1093/gji/ggt482>, 2014.

419 Shi, F., Wang, X. C., and YUN L.: *Matlab neural network case study*, The Beijing University of Aeronautics &
420 Astronautics Press, Beijing, 2010.

421 Sharma, S. P.: VFSARES—a very fast simulated annealing FORTRAN program for interpretation of 1-D DC
422 resistivity sounding data from various electrode arrays, *Comput. Geosci.*, 42, 177-188,
423 <https://doi.org/10.1016/j.cageo.2011.08.029>, 2012.

424 Shi, X. M., Xiao, M., Fan, J. K., Yang, G. S., and Zhang, X. H.: The damped PSO algorithm and its application for
425 magnetotelluric sounding data inversion, *Chinese Journal of Geophysics.*, 52, 1114–1120,
426 <https://doi.org/10.3969/j.issn.0001-5733.2009.04.029>, 2009.

427 Srinivas, Y., Raj, A. S., Oliver, D. H., Muthuraj, D., and Chandrasekar, N.: A robust behavior of Feed Forward
428 Back propagation algorithm of Artificial Neural Networks in the application of vertical electrical sounding data

429 inversion, *Geosci. Front.*, 3, 729-736, <https://doi.org/10.1016/j.gsf.2012.02.003>, 2012.

430 Tran, K. T., and Hiltunen, D. R.: Two-Dimensional Inversion of Full Waveforms Using Simulated Annealing, *J.*
431 *Geotech. Geoenviron. Eng.*, 138, <https://doi.org/1075-1090>, 2012.

432 Li, Y. Y., Chen, B. C., Zhao, Y. G., Yun, C., Ma, X. B., and Kong, X. R.: Nonlinear inversion for electrical
433 resistivity tomography, *Chinese Journal of Geophysics*, 52, 758-764,
434 [https://doi.org/10.1016/S1003-6326\(09\)60084-4](https://doi.org/10.1016/S1003-6326(09)60084-4), 2009.

435 Zhang, L. Y., and Liu, H. F.: The application of ABP method in high-density resistivity method inversion, *Chinese*
436 *Journal of Geophysics.*, 54, 64-71, <https://doi.org/10.1002/cjg2.1587>, 2011.